Vibration Isolation of Asymmetric Rigid Plate Using One and Pair Pre-bent Strut at Each Corner under Static and Dynamic Axial Excitation

Aly El-Kafrawy
Port-Said University Department of Production Engineering and Machine Design
Port- Said, ARE
dr_eng_aly@hotmail.com

Anwar Kandil
Port-Said University Department of Production Engineering and Machine Design
Port- Said, ARE
anwarkandil@hotmail.com

Mostafa Helaly
Alexandria University Department of Production Engineering
Faculty of Engineering, ARE Alexandria,
mohelaly@globalnet.com

Abu-Bakr Omar
Suez Canal University Department of Production Engineering and Machine Design
Ismailia, ARE
abubakr31869@yahoo.com

ABSTRACT

This paper is concerned with the influence of vibration isolators in the form of post-buckled elastic clamped-clamped one and pair strut to relief the vibrating machines from the harmful effects of vibration. These vibrations are in most cases uncontrollable and lead to sudden failure, therefore, mechanical engineers in preventive maintenance sections have to control, isolate, and minimize the harmful effects of such unwanted vibrations. A mathematical model consists of pre-bent post-buckled one and pair strut acting as vibration isolators supporting an asymmetric rigid plate. The model is subject to axial harmonic excitation at the base, and allowed to displace laterally with respect to axial center line of the isolated plate. The displacement transmissibility is calculated over a wide range of frequencies and plotted in form of design charts. The transmissibility plots are used to recognize the ranges of frequencies, at which isolation can be maintained. The resonance frequencies of the system can be easily depicted from the design graphs. The present study reveals that at resonance frequencies the most effective transmissibility is well below unity. Vibration characteristics are determined under specific frequencies such that the physical behavior of the system can be thoroughly analyzed. All variables used in the analysis are normalized, such that the results aren't dependent on any material or geometric property. In this way, the obtained results can be applied over a wide range of elastic materials, regardless of the type of material or section properties.

Keywords Transmissibility, Euler elastic buckling, Vibration isolation, Struts, asymmetric rigid plate, post-buckled

عزل الإهتزازات لمستوى جاسيء غير متماثل باستخدام عازل واحد وكذا زوج من العوازل من أذرع مرنة منبعجة مسبقا متعرضا إلى إثارة محورية إستاتيكية وديناميكية

الهدف من هذا البحث هو دراسة تأثير استخدام عوازل للإهتزازات التي على شكل أذرع مرنه منحنية ومثبت أحد طرفيها بالجسم المراد عزله والآخر بالق اعدة المثبت عليها الجسم ، وذلك لتجنب التأثيرات الضارة للإهتزازات على الماكينات . هذه الإهتزازات تكون في معظم الحالات غير مسيطر عليها وتؤدى إلى انهيار مفاجئ و بالتالي خسارة للماكينات . لذلك فإن المهندسين الميكانيكيين في أقسام الصيانة الوقائية في مجال الصناعة يعملون بجدية لوضع هذه الاهتزازا ت تحت السيطرة وعزل وتقليل الآثار الضارة لها. ويقدم هذا البحث نموذج رياضي مكون من مستوى جاسيء غير مت ماثل معلق عن طريق ذراع واحد منحنى مرن منبعج مسبقا وكذلك ذراعين كعوازل للاهتزازات . ويتعرض هذا الموديل لإثارة هرمونية محورية عند القاعدة ويسمح الموديل بحركة إنتقالية عرضية بالنسبة لمحور المستوى المعزول. إن نسبة الإنتقالية للإزاحة تعتبر العنصر المنظم لكفاءة العازل فى عزل الإهتزازات المنتقلة من القاعدة إلى الجسم الجاسئ . وتحسب نسبة الإنتقالية عبر مدى واسع من الترددات و ترسم كمنحنيات تصميمية لتحديد تأثيرها على سلوك الإهتزازات باستخدام تلك العوازل. وقد أعطيت درجة حرية اضافية وهى السماح بالحركة الإنتقالية للمستوى المعزول . وتستخدم رسومات الإنتقالية للتعرف على مدى الترددات الذى عنده يمكن تحقيق العزل . ويمكن عندئذ تحديد ترددات الرنين للنظام من الرسومات المصممه . وقد أظهرت هذه الدراسة أنه عند ترددات الرنين تكون نسبة الإنتقالية الأكثر كفاءة عند قيمة أقل من الواحد. إن سمات الإهتزازات يتم تحديدها عند ترددات معينة بحيث أن السلوك الطبيعي للنظام يمكن تحليله من خلال ذلك . كل المتغيرات المستخدمة فى التحليل هى بدون أبعاد وبذلك فإن هذه النتائج لا تعتمد على خواص أى مادة أو شكل هندسى معين مثل معامل المرونه للمادة ومعامل المقط ع للشكل المستخدم أو طول العازل. وبهذه الطريقة يمكن تطبيق النتائج المستخلصة على مدى واسع من المواد المرنه بغض النظر عن نوع المادة أو خواص المقطع . وقد اتضح أن اتجاه الإنحناء للأذرع المنبعجة نحو اليسار أو اليمين ليس له تأثير على عزم الإتزان وقوى القص وبالتالى على نسبة ا لإنتقالية. يمكن تحسين عزل الإهتزازات باستخدام الأذرع المنبعجة حتى فى وجود حركة انتقالية عرضية للجسم المراد عزله . وتساعد الحركة الإنتقالية العرضية على تحسين قيمة نسبة الإنتقالية وبالتالى كفاءة العزل خاصة عند الترددات المنخفضة. ان استخدام زوج من الأذرع المنبعجة يحسن قيم نسبة الإنتقالية عن استخدام ذراع واحد عند الترددات المنخفضة وهذا لايتحقق مع الترددات العالية. تتغير قيم نسبة الإنتقالية مع تغير موضع مركز الكتلة للجسم المعزول.

1. Introduction and literature review

Several modern machinery, such as compressors, internal combustion engines, mining machines, hydraulic, and pneumatic presses, turbo machinery, etc. undergo uncomfortable and even undesirable serious source. These vibrations are in most cases uncontrollable and lead to sudden failure and in turn to a loss of machines availability. Therefore, mechanical engineers in preventive maintenance sections in the industry have the serious job to put these vibrations under control, isolate, and minimize the harmful effects of such unwanted vibrations.

Hoque et al. (2010) developed the vibration isolation system fundamentally, by connecting an active negative suspension realized by zero-power control in series with an active–passive positive suspension. The system could effectively isolate ground vibrations in addition to suppress the effect of on-board generated direct disturbances of the six-axis motions, associated with vertical and horizontal directions. Yun, Y., Mak, C.M. (2010) used the level of ''power transmissibility'' to assess the performance of vibration isolators, and the level of the ''vibration velocity transmissibility'' of the supporting floor structure, the ''mounted vibration velocity'', and the ''mounted rotational velocity level'' of the vibratory machine were proposed to assess the stability of the vibratory system with various inertia blocks. The results primarily have indicated that the use of an inertia block did not affect the performance of vibration isolation. Leo, D.J. and Inman (1999) used a quadratic programming algorithm for studying the design tradeoffs of active-passive vibration isolation systems

In Carrellaa et al. (2009), the force transmissibility of a quasi-zero-stiffness (QZS) isolator was considered. The isolator comprised a vertical spring and two oblique springs that were either linear, linear with pre-stress or softening nonlinear with pre-stress. Carrellaa et al. (2008) proposed a theoretical and experimental study of one such mount stiffness required to support a static load. It comprised two vertical mechanical springs between which an isolated mass was mounted. Lee et al. (2007) presented an approach, based on the consistent theory of thin shells, for designing compact springs in terms of their compatibility with the room available for packaging the vehicle suspensions and simultaneous extension of the height control region where fundamental frequencies were kept minimal. Jalili, N. (2000) presented the development of an innovative approach for optimum vibration suppression of flexible structures. It was shown that concurrent adjustment of structural properties and control re-tuning significantly improved the vibration suppression quality.

Mizuno et al. (2007) studied analytically and experimentally an active vibration isolation system using zero-power magnetic suspension. Yilmaz et al. (2006) aimed to design a stiff and lightweight passive vibration isolator that had wide stopband at low frequencies. First of all, bandwidths of single-degree-of-freedom (sdof) dynamic vibration absorbers and lever-type anti-resonant vibration isolators were formulated in a general framework. Then, by making use of these formulations, a 2dof vibration isolator was synthesized to obtain large bandwidth at low frequencies. Winthropa et al. (2005) developed a method for selecting and understanding the performance of variable stiffness devices. The exact solution was used to create an approximate solution directly linking past variable stiffness approximations to the exact solution in a systematic way. Bai et al. (2002) presented numerical and experimental investigations on active vibration isolation system. Two configurations were implemented for a statically balanced three-mount system. Roh, J.H. (2008) applied the shape memory alloys (SMAs) as actuators and vibration isolation devices.

2. Equilibrium analysis

Equilibrium analysis procedure

The model studied in this paper is a simple system consisting of four buckled struts used to support an asymmetric rigid plate and is limited for non-dimensionalized frequencies of up to 200. The analysis of buckled struts as vibration isolators is based on the use of four struts connected by a rigid plate at four corners (Jeffers et al. 2005). Jeffers et al. (2005), Alloway (2003), and Plaut et al. (2003) have used strut elements as isolators for fixed-fixed bars underlying axial harmonic displacement excitation. Sidburg (2003) has used the same isolators as used in Jeffers et al. (2005), Alloway (2003), and Plaut et al. (2003) with pinned-pinned end condition. The author of the present work has used the same type of isolators as that used in Jeffers et al. (2005), Alloway (2003), Plaut et al. (2003), and Sidburg (2003). However, the end condition is selected within the present analysis as clamped - clamped. El-Kafrawy, A. et al. (4 May 2010) studied the vibration isolation of a symmetric and asymmetric rigid bar using struts subject to axial static and dynamic excitation. El-Kafrawy, A. et al. (28 September 2010) treated the case of the vibration isolation of a symmetric rigid plate using struts subject to axial static and dynamic excitation.

The results determined in Jeffers et al. (2005), Alloway (2003), Plaut et al. (2003), Sidburg (2003), and El-Kafrawy, A. et al. (28 September 2010) revealed that the behavior of the buckled strut under axial, harmonic, displacement excitation is similar for both fixed-fixed

and pinned-pinned end conditions. In the present paper it has been decided to choose fixed-fixed end conditions, since such system can support much higher load.

The first step in the analysis is to evaluate the model at static equilibrium for the plate. In the second step the strut is analyzed in a post buckled state, with clamped-clamped ends as done by Jeffers et al. (2005) and Virgin and Davis (2003) as shown in Fig. 1. It should be noted that the model is constrained against any lateral movement except in $\overline{Y}$-direction. If the analyzed model is free to move laterally, the model consisting of pre-bent struts may become unstable and would buckle and sway (Inman 1994).

Rigid plate analysis
The plate analyzed in the present work is symmetric. It has the ability to move vertically, rotate about the $\overline{X}$ and $\overline{Y}$ axes and allowed to move laterally in direction-$\overline{Y}$ as shown in Fig. 1. The horizontal movements at the corners of the plate due to such rotations will be ignored in the equilibrium analysis because only small rotations of the plate will be considered. As a result, the plate will be analyzed as a four degree-of-freedom system.

Upon considering the free body diagram of the plate shown in Fig. 2, one apparent observation is that there are four unknown forces, F_1, F_2, F_3 and F_4, acting at the corners of the plate, but only four equations result from the equilibrium. These equations are:
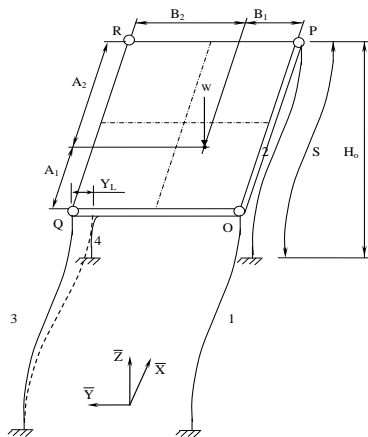
$$F_1 + F_2 + F_3 + F_4 = W \qquad (1)$$
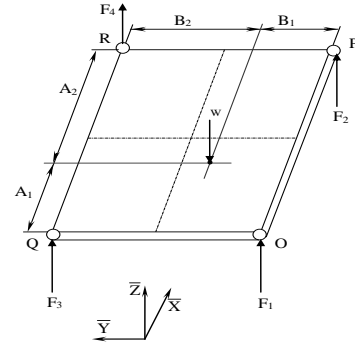$$-(F_1 + F_2)B_1 + (F_3 + F_4)B_2 = 0 \qquad (2)$$
$$(F_1 + F_3)A_1 - (F_2 + F_4)A_2 = 0 \qquad (3)$$
$$Z_O - Z_P - Z_Q + Z_R = 0 \qquad (4)$$

Where: Z_O, Z_P, Z_Q, and Z_R are the vertical displacements at the corners of the plate, which are labeled by O, P, Q, and R when it rotates at some angle about $\overline{X}$ and $\overline{Y}$ axes.

**Fig. 1 Asymmetric rigid plate supported by pre-bent one strut at each corner**

**Fig. 2 Free-body diagram of the plate in static equilibrium state**

Vibration Isolator Analysis
Now that the axial force applied to the top of each isolator can be determined, it is necessary to examine the force-displacement relationship for each isolator. As stated earlier, the isolator, shown horizontally in Fig.3, consists of one strut which is clamped at both ends. For simplicity, the isolator is restrained against rotation at both ends and free horizontal ($\overline{Y}$-direction) displacement without any external laterally force in this direction.

The additional variables used for the remaining portion of this analysis can be defined as follows. The subscript st is used for static equilibrium analysis. Note that the subscript i is used to denote the current number of isolators. The struts have the same length and bending stiffness. Hence, the analysis is only carried out on one strut. The other struts represent actually a typical and mirror image of the first. A free-body diagram of an incremental element of the strut is shown in Fig. 4. Under the existing load on the isolator, F_i, the strut deflects from the initial configuration to a new position $Y_{i,st}(S)$. The following equations are derived to describe the shape of the strut:
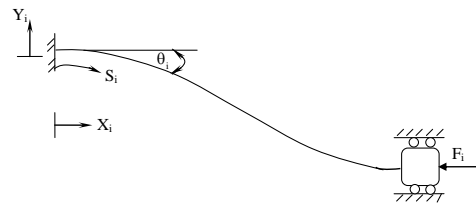
Fig. 3 Model of vibration isolator under static axial load F_i
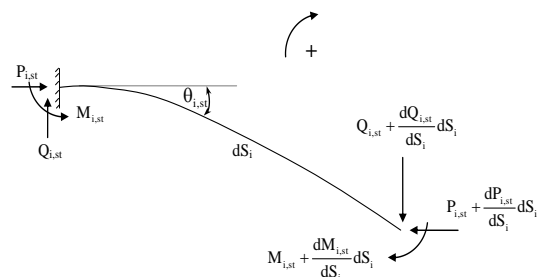
Fig. 4 Free body diagram of an element of the strut

15

$$\cos\theta_{i,st} = \frac{dX_{i,st}}{dS_i} \qquad (5)$$

$$\sin\theta_{i,st} = -\frac{dY_{i,st}}{dS_i} \qquad (6)$$

$$\frac{d\theta_{i,st}}{dS_i} = -\frac{M_{i,st}}{\beta_i EI} \qquad (7)$$

$$\frac{dM_{i,st}}{dS_i} = P_{i,st}\sin\theta_{i,st} + Q_{i,st}\cos\theta_{i,st} \qquad (8)$$

The struts are made of an elastic material to support a static load up to the critical point, at which the strut buckles. This critical point is known as the Euler buckling load and its value depends upon the support end conditions. For a fixed-fixed strut (not allowed to rotate or to deflect transversely) the critical load is given by $P_{cr} = 4\pi^2 EI/L^2$. For a pinned-pinned strut (free to rotate transversely) the critical load is given by $P_{cr} = \pi^2 EI/L^2$ (Inman 1994). The variables have been normalized so that the analysis provides relevant results for any elastic material, regardless of its geometric and material properties.

Note that the bending stiffness EI for each strut is multiplied by a modification factor β_i. The stiffness modification factors will be chosen so that the downward deflection at the top of each strut due to the static load F_i is the same for all four isolators. In other words, each isolator will have the same initial height H_o when the system is in equilibrium. Because of symmetry, the axial force $P_{i,st}$ in the strut is equal to the total load F_i applied to the isolator. That is,

$$F_i = P_{i,st} \qquad (9)$$

Equations 5–8 lead to the following differential equations (for $0 \le s \le 1$).

$$\cos\theta_{i,st} = \frac{dx_{i,st}}{ds_i} \qquad (10)$$

$$-\sin\theta_{i,st} = \frac{dy_{i,st}}{ds_i} \qquad (11)$$

$$\frac{d\theta_{i,st}}{ds_i} = -\frac{m_{i,st}}{\beta_i} \qquad (12)$$

$$\frac{dm_{i,st}}{ds_i} = p_{i,st}\sin\theta_{i,st} + q_{i,st}\cos\theta_{i,st} \qquad (13)$$

The boundary conditions must be established to complement the differential Equations 10–13. The fixed-fixed end condition of the strut does not allow any rotation at its ends, but it allows only small deflection (lateral movement) in the $\overline{Y}$-direction, Fig. 1.

Boundary conditions for static equilibrium state
The boundary conditions of the treated model in static equilibrium state can be written as follows:

At $s_{i,st} = 0$; $\quad x_{i,st} = 0$, $\quad y_{i,st} = 0$, and $\quad \theta_{i,st} = 0$

(the left, or bottom, end of the strut)

At $s_{i,st} = 1$; $\quad y_{1,st} = y_{3,st}$, $\quad y_{2,st} = y_{4,st}$ and $\quad \theta_{i,st} = 0$

(the right, or top, end of the strut)

Recall that Eq. 4 is still in terms of the total forces applied to the isolator rather than the axial forces in each strut. Furthermore, Eq. 4 is in terms of the displacements at the corners of the plate. From continuity, the vertical displacement at a given corner is equal to the $\overline{X}$-direction displacement at the end of the strut of the isolator attached at that corner. Specifically, $Z_O = X_{1,st}(L)$, $Z_P = X_{2,st}(L)$, $Z_Q = X_{3,st}(L)$ and $Z_R = X_{4,st}(L)$. Substituting these relationships into Eq. 4, the following equations ensue:

$$p_{1,st} + p_{2,st} + p_{3,st} + p_{4,st} = w \qquad (14)$$

$$-(p_{1,st} + p_{2,st})b_1 + (p_{3,st} + p_{4,st})b_2 = 0 \qquad (15)$$

$$(p_{1,st} + p_{3,st})a_1 - (p_{2,st} + p_{4,st})a_2 = 0 \qquad (16)$$

$$x_{1,st}(1) - x_{2,st}(1) - x_{3,st}(1) + x_{4,st}(1) = 0 \qquad (17)$$

A computer program has been implemented as an interface to Mathematica, Ver. 5.2 (Wolfram Research, Inc. 2005) to solve the system of differential Equations (10-13). Based on the given initial value of load, p_o, the implemented program solves for the value of the moment, m at the left end, or bottom, of the strut (s=0). Because of the nonlinearity of the system of equations, the solution is based on an iterative algorithm making use of the shooting method. The iteration is based on an initial guess for the moment, m.

3. Dynamic Analysis

Dynamic Analysis Procedure
Within the dynamic model the symmetric plate is assumed to be subject to a forced axial harmonic vibration as per (Den Hartog 1985) (axial base displacement). as shown in Fig. 5. Similar to the static equilibrium analysis, the derivation of the equations of motion for the dynamic analysis is also divided into two parts. First, the equations of motion for the rigid plate are determined from the kinetic and potential energies in the system using Lagrange's equations. Second, the strut in each isolator is analyzed using D'Alembert's principle. All dynamic equations are linearized for small motions and put in non-dimensional form. A program written in Mathematica is used to numerically solve these equations to determine the motion transmissibility of the system.

Rigid plate analysis
The $\overline{X}, \overline{Y}, \overline{Z}$ coordinate system is fixed in space as shown in Fig. 6 and has unit vectors $\hat{i}, \hat{j}$ and $\hat{k}$. The angles θ, ψ and ϕ are used to define coordinate rotations about the $\overline{X}, -\overline{Y}$ and $\overline{Z}$ axes, respectively, and are initially zero. The points O, P, Q, and R are located at the bottom of each corner of the plate, and the plate has an initial

height H_o when the system is in static equilibrium state. The center of mass (labeled c.m. in Fig. 6) is indicated by the dimensions A_1, A_2, B_1, and B_2, and it is positioned at a distance C^c above the bottom of the plate.

The equations of motion for the plate will be determined using Lagrange's equations. Thus, it is necessary to determine the kinetic and potential energies of all components of the system. Because it is desirable to preserve symmetry in the model for the vibration isolator, horizontal springs are added to the corners of the plate to simulate the horizontal resistance contributed by the isolators when the plate rotates. Because this horizontal motion is very small, this assumption should have a minimal effect on the results of this analysis. The springs are numbered $1 - 8$ and attach to the plate.
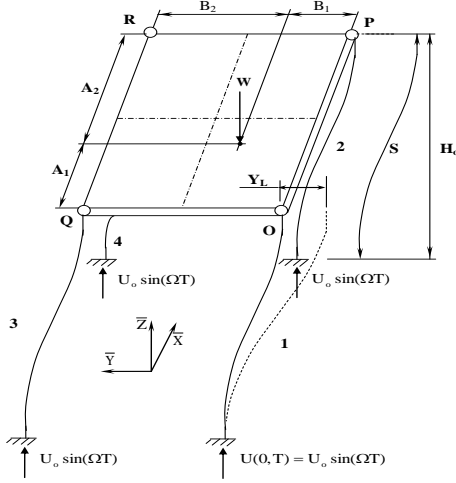
Fig. 5 The components of model for the dynamic state
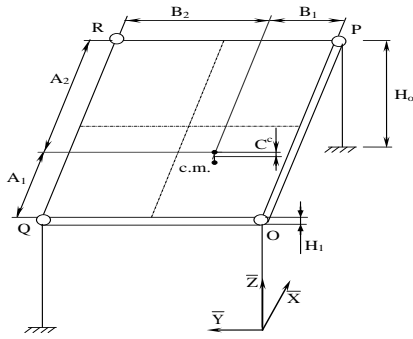
Fig. 6 Initial configuration of the plate

The plate has both rotational and translational kinetic energy. The equations of motion for the plate become:

$$Y_{Q,d} = Y_{O,d} \tag{18}$$

$$X_{P,d} = X_{O,d} \tag{19}$$

$$\frac{-M\Omega^2}{A_1 + A_2}[A_2 X_{O,d} + A_1 X_{P,d} - C^c X_{2,d}(L) +$$

$$C^c X_{1,d}(L)] + (K_2 + K_3)X_{P,d} + (K_6 + K_7)X_{O,d} = 0 \tag{20}$$

$$\frac{-M\Omega^2}{B_1 + B_2}[B_1 Y_{Q,d} + B_2 Y_{O,d} - C^c X_{3,d}(L) +$$

$$C^c X_{1,d}(L)] + (K_1 + K_8)Y_{O,d} + (K_4 + K_5)Y_{Q,d} = 0 \tag{21}$$

$$\frac{-M\Omega^2}{A_1 + A_2}[A_1 X_{2,d}(L) + A_2 X_{1,d}(L) + C^c X_{P,d} - C^c X_{O,d}] -$$

$$\frac{M\Omega^2}{A_1 + A_2}[B_1 X_{3,d}(L) - B_1 X_{1,d}(L) + C^c Y_{Q,d} - C^c X_{O,d}]$$

$$= P_{1,d}(L) + P_{2,d}(L) + P_{3,d}(L) + P_{4,d}(L) \tag{22}$$

$$\frac{-I_X \Omega^2}{B_1 + B_2}[X_{3,d}(L) - X_{1,d}(L)]$$

$$= -[P_{1,d}(L) + P_{2,d}(L)]B_1 + [P_{3,d}(L) + P_{4,d}(L)]B_2 \tag{23}$$

$$\frac{-I_Y \Omega^2}{A_1 + A_2}[X_{2,d}(L) - X_{1,d}(L)]$$

$$= -[P_{1,d}(L) + P_{3,d}(L)]A_1 + [P_{2,d}(L) + P_{4,d}(L)]A_2 \tag{24}$$

Calculation of the mass moment of inertia for the asymmetric plate

For the purpose of calculating the mass moment of inertia, the eccentricity of the plate will be modeled as a block set on top of the plate, where the block is positioned arbitrarily on top of the plate, as shown in Fig. 7. This model is representative of a piece of equipment set on top of the rigid plate. The plate has a thickness H_1 and the block has a height H_2 and width and depth D. The center of mass for the combination of the plate and block is given by the dimensions A_1, A_2, B_1, B_2, and C^c, where A_1 and A_2 give the position of the center of mass along the $\overline{X}$-axis, B1 and B2 give the position of the center of mass along the $-\overline{Y}$-axis, C^c gives the position of the center of mass in the $\overline{Z}$ direction measured from the bottom of the plate, as shown in Figs. 6-7.
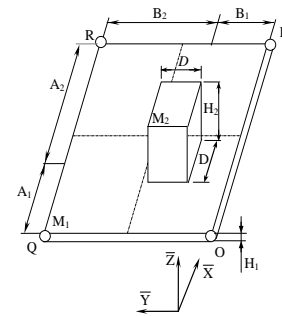
Fig. 7 Dimensions of block on top of asymmetric rigid plate

The values for A_1, A_2, B_1, and B_2 are known and are specified directly. However, C^c must be calculated in terms of the dimensions of the block and the plate using the following equation :

$$C^c = \frac{\sum \tilde{Z}A}{\sum A} \tag{25}$$

$$C^c = \frac{(A_1 + A_2)H_1 * \dfrac{H_1}{2} + DH_2\left(H_1 + \dfrac{H_2}{2}\right)}{(A_1 + A_2)H_1 + DH_2} \qquad (26)$$

Assuming that the plate has mass M_1, the mass moments of inertia about the $\overline{X}$ and $\overline{Y}$ axes at the center of mass can be calculated as follows:

$$I_X = \frac{M_1}{12}\left[(B_1 + B_2)^2 + H_1{}^2\right] + M_1\left(\frac{B_1 + B_2}{2} - B_1\right)^2$$

$$+ M_1\left(\frac{H_1}{2} - C^c\right)^2 + \frac{M_2}{12}\left[D^2 + H_2{}^2\right]$$

$$+ M_2\left(\frac{B_1(B_1 + B_2)H_1 - (B_1 + B_2)^2\dfrac{H_1}{2}}{DH_2}\right)^2 +$$

$$M_2\left(H_1 + \frac{H_2}{2} - C^c\right)^2 \qquad (27)$$

$$I_Y = \frac{M_1}{12}\left[(A_1 + A_2)^2 + H_1{}^2\right] + M_1\left(\frac{A_1 + A_2}{2} - A_1\right)^2$$

$$+ M_1\left(\frac{H_1}{2} - C^c\right)^2 + \frac{M_2}{12}\left[D^2 + H_2{}^2\right]$$

$$+ M_2\left(\frac{A_1(A_1 + A_2)H_1 - (A_1 + A_2)^2\dfrac{H_1}{2}}{DH_2}\right)^2 +$$

$$M_2\left(H_1 + \frac{H_2}{2} - C^c\right)^2 \qquad (28)$$

Analysis of the vibration isolator

In Den Hartog (1985) as well as in the present work the strut is assumed to take a horizontal position as shown in Fig. 8, such that the base lies at the left side of strut, at which the excitation force acts. Fig. 8 shows the isolator subjected to a harmonic base excitation U(T), where U(T) was defined as $U(T) = U_o \sin(\Omega T)$. This imposed base displacement is resisted at the top of the isolator by the force F_i, which is now a portion of the combined effects of the weight W of the plate and the inertial load from the mass of the plate. In the analysis of the vibration isolator, it is again assumed that the horizontal movements $X_{O,d}$, $X_{P,d}$, $X_{Q,d}$, $X_{R,d}$, $Y_{O,d}$, $Y_{P,d}$, $Y_{Q,d}$, and $Y_{R,d}$ (generated by rotation angle θ about $\overline{X}$-axis and angle ψ about $-\overline{Y}$-axis)at the corners of the plate are small enough that they can be neglected and symmetry can be used in the analysis of each isolator. It can be noticed that the deflection is a function of position along the strut, L and time, T.
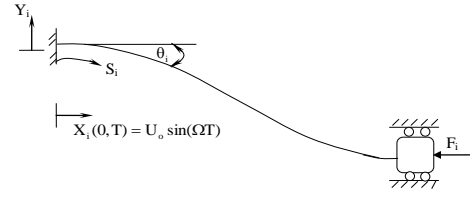

Fig. 8 Strut under forced harmonic vibration

In the present case we deal with linear viscous damping, i.e., the relationship between the damping force and the velocity of the system is linear. The analysis revealed that damping has a negligible effect on the transmissibility. The damping effect cannot be determined from geometrical, material, or other physical properties of the strut element. Hence, the damping effect can be determined through experiments such as a free vibration test. In any case, damping is present and must be taken into account.

To analyze the strut under forced harmonic excitation, a free body diagram of forces acting on an element at a particular time and position should be considered as shown in Fig. 9. This can be done by making use of D'Alembert's Principle, which is based on a fictitious inertia force that is set equal to the product of the mass and the acceleration. This force is assumed to act in the opposite direction of the accelerating mass. Hence, at any particular instant, the strut is considered to be in a state of static equilibrium (Chopra 2001).

Notice that the mass per unit length μ of the strut is multiplied by the factor β_i that was used to adjust the bending stiffness EI in the equilibrium analysis. Assuming that the same material is used in each strut (i.e., the modulus of elasticity E remains constant), the bending stiffness can be modified by changing the cross-section of the strut so that the moment of inertia about the axis of bending becomes $\beta_i I$.

From the geometry, equilibrium, and the elastic constitutive laws for the strut, the following relationships can be established for the strut subjected to forced harmonic vibrations. The governing variables describing the strut can now be written as a function of time and location along the strut to describe the response of the strut to the forced excitation. The subscript "st" represents the static equilibrium portion of the equation, and "d" represents the dynamic portion, these equations are written below:
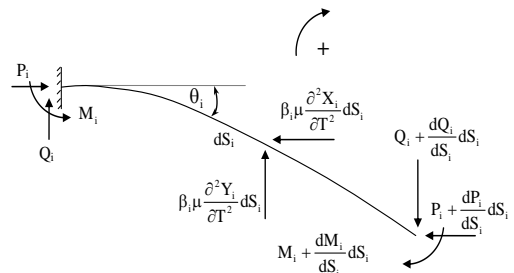
$$\frac{dX_{i,d}}{dS_i} = -\theta_{i,d}\sin\theta_{i,st} \quad (29)$$

$$\frac{dY_{i,d}}{dS_i} = -\theta_{i,d}\cos\theta_{i,st} \quad (30)$$

$$\frac{d\theta_{i,d}}{dS_i} = -\frac{M_{i,d}}{\beta_i EI} \quad (31)$$

$$\frac{dM_{i,d}}{dS_i} = (Q_{i,d} + P_{i,st}\theta_{i,d})\cos\theta_{i,st}$$
$$+ (P_{i,d} - Q_{i,st}\theta_{i,d})\sin\theta_{i,st} \quad (32)$$

$$\frac{dP_{i,d}}{dS_i} = \beta_i\mu\Omega^2 X_{i,d} \quad (33)$$

$$\frac{dQ_{i,d}}{dS_i} = \beta_i\mu\Omega^2 Y_{i,d} \quad (34)$$

The variables describing the strut can now be written as a function of time and location along the strut to describe the response of the strut to the forced excitation. It is assumed that the dynamic vibrations will be relatively small. Hence, small displacement theory can be used to derive the following linear dynamic relationships. These equations are written below in non-dimensional form:

$$y_{Q,d} = y_{O,d} \quad (35)$$

$$x_{P,d} = x_{O,d} \quad (36)$$

The equations of motion for the plate can be written as:

$$-rw\omega^2[a_2 x_{O,d} + a_1 x_{P,d} - c^c x_{2,d}(l) +$$
$$c^c x_{1,d}(l)] + (k_2 + k_3)x_{P,d} + (k_6 + k_7)x_{O,d} = 0 \quad (37)$$

$$\frac{-rw\omega^2}{\alpha}[b_1 y_{Q,d} + b_2 y_{O,d} - c^c x_{3,d}(l) +$$
$$c^c x_{1,d}(l)] + (k_1 + k_8)y_{O,d} + (k_4 + k_5)y_{Q,d} = 0 \quad (38)$$

$$-rw\omega^2[a_1 x_{2,d}(l) + a_2 x_{1,d}(l) + c^c x_{P,d} - c^c x_{O,d}]$$
$$-\frac{rw\omega^2}{\alpha}[b_1 x_{3,d}(l) - b_1 x_{1,d}(l) + c^c y_{Q,d} - c^c y_{O,d}]$$
$$= p_{1,d}(l) + p_{2,d}(l) + p_{3,d}(l) + p_{4,d}(l) \quad (39)$$

$$\frac{-i_x\omega^2}{\alpha}[x_{3,d}(l) - x_{1,d}(l)]$$
$$= -[p_{1,d}(l) + p_{2,d}(l)]b_1 + [p_{3,d}(l) + p_{4,d}(l)]b_2 \quad (40)$$

$$-i_y\omega^2[x_{2,d}(l) - x_{1,d}(l)]$$
$$= -[p_{1,d}(l) + p_{3,d}(l)]a_1 + [p_{2,d}(l) + p_{4,d}(l)]a_2 \quad (41)$$

The mass moments of inertia become the form:

$$i_x = m_1\left\{\frac{1}{12}\left[\alpha^2 + h_1^2\right] + \left[\left(\frac{\alpha}{2} - b_1\right)^2 + \left(\frac{h_1}{2} - c^c\right)^2\right]\right\}$$
$$+ \frac{m_2}{12}\left[d^2 + h_2^2\right] + m_2\left(\frac{\alpha b_1 h_1 - \alpha^2\frac{h_1}{2}}{dh_2}\right)^2$$
$$+ m_2\left(h_1 + \frac{h_2}{2} - c^c\right)^2 \quad (42)$$

$$i_y = m_1\left\{\frac{1}{12}\left[1 + h_1^2\right] + \left[\left(\frac{1}{2} - a_1\right)^2 + \left(\frac{h_1}{2} - c^c\right)^2\right]\right\}$$
$$+ \frac{m_2}{12}\left[d^2 + h_2^2\right] + m_2\left(\frac{a_1 h_1 - \frac{h_1}{2}}{dh_2}\right)^2$$
$$+ m_2\left(h_1 + \frac{h_2}{2} - c^c\right)^2 \quad (43)$$

$$c^c = \frac{\frac{h_1^2}{2} + dh_2\left(h_1 + \frac{h_2}{2}\right)}{h_1 + dh_2} \quad (44)$$

Similarly, the dynamic equations for the strut can be written as:

$$\frac{dx_{i,d}}{ds_i} = -\theta_{i,d}\sin\theta_{i,st} \quad (45)$$

$$\frac{dy_{i,d}}{ds_i} = -\theta_{i,d}\cos\theta_{i,st} \quad (46)$$

$$\frac{d\theta_{i,d}}{ds_i} = -\frac{m_{i,d}}{\beta_i} \quad (47)$$

$$\frac{dm_{i,d}}{ds_i} = (q_{i,d} + p_{i,st}\theta_{i,d})\cos\theta_{i,st}$$
$$+ (p_{i,d} - q_{i,st}\theta_{i,d})\sin\theta_{i,st} \quad (48)$$

$$\frac{dp_{i,d}}{ds_i} = \beta_i\omega^2 x_{i,d} \quad (49)$$

$$\frac{dq_{i,d}}{ds_i} = \beta_i\omega^2 y_{i,d} \quad (50)$$

The boundary conditions for dynamic state

The boundary conditions at each end of the strut can be written in a non-dimensional form:

At $s_i = 0$; $x_{i,d} = u_o$, $y_{i,d} = 0$, and $\theta_{i,d} = 0$

At $s_i = 1$; $y_{1,d} = y_{3,d}$, $y_{2,d} = y_{4,d}$, $y_{2,d} = y_{3,d}$, $y_{1,d} = y_{4,d}$, and
$\theta_{i,d} = 0$

Similar to the static solution, the governing differential equations can be implemented in Mathematica to solve for the dynamic transmissibility. The moment m_{st} determined from the equilibrium analysis is used as initial value in the dynamic analysis to

19

determine the dynamic transmissibility. Other known values of the initial load p_o, the amplitude of excitation at the base u_o, the stiffness parameter, r, and the external damping parameter, c, are defined and used as input in the program. Repeatedly, the iterative scheme based on the use of the shooting method is implemented to solve the equations; with the following initial variables $p_d(0)$, $q_d(0)$, and $m_d(0)$. To increase the convergence, the resulting variables: $p_d(0)$, $q_d(0)$, and $m_d(0)$, are updated by adding weighted percentage of their initial values, are then used as a guess for the next iteration in the loop.

The dynamic transmissibility of the system is the ultimate goal of this work. The equations used to determine the transmissibility is given below. As mentioned before, we deal herein with a displacement transmissibility. The implemented algorithm is programmed again by Mathematica to solve for the real and imaginary parts of the solution.

$$TR_i = \frac{\sqrt{\{Re[x_{i,d}(l)]\}^2 + \{Im[x_{i,d}(l)]\}^2}}{|u_o|} \qquad (51)$$

$$TR = \frac{TR_1 + TR_2 + TR_3 + TR_4}{4} \qquad (52)$$

The square root of the sum of the squares (SRSS) of the real and imaginary eigen values are used to calculate the displacement of the strut at the top under the acting dynamic load. The SRSS is then divided by the original amplitude of the base, u_o, to determine the dynamic transmissibility. Because each strut underlies the same amplitude and frequency, the dynamic transmissibility calculated at the top of each strut is the same at the center of the rigid plate.

4. Results and discussion

Using the Mathematica program, the equations of motion derived in this research for the system are numerically solved. The system is analyzed for the asymmetric case, i.e., First, the center of mass is positioned at several points along a line that runs through the center of the plate perpendicular to the edge OP of the plate, as shown in Fig. 10-a. Secondly, the center of mass is positioned at several points along a line of symmetry that passes diagonally from corner R to corner O, as shown in Fig. 10-b.

The transmissibility is computed and plotted for a wide range of non-dimensional excitation frequencies for each of these cases. The transmissibility plots are used to recognize frequencies at which resonance occurs in the system and frequency ranges in which the transmissibility is small.
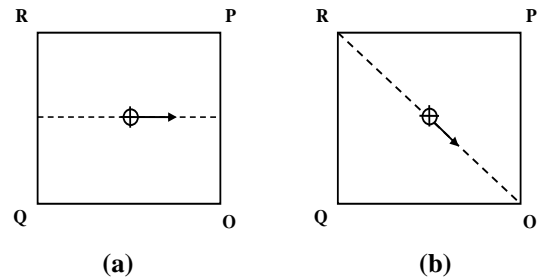
(a)   **(b)**
Fig. 10 Location of the center of mass of plate for (a) case 1 and (b) case 2

The equations of motion are solved for the case shown in Fig. 10. The non-dimensional weight w is set at 160, as was done in the equilibrium analysis. Similarly, the stiffness k_j of the eight horizontal springs attached to the plate is each set at 0.1 as shown in Fig. 11. The aspect ratio α of the plate is set equal to 1, i.e. the plate remains square in this analysis. The plate dimension h_1, required to calculate the vertical distance c^c to the center of mass and the mass moments of inertia, i_x and i_y, are set equal to 0.05. The stiffness modification factor β_i and the equilibrium portion of the axial force $p_{i,st}$, the shear force $q_{i,st}$, and the bending moment $m_{i,st}$ for each strut are obtained from the equilibrium analysis. From the solution of the equations of motion, the transmissibility TR is calculated for various excitation frequencies ω using Eqns. (51 and 52).
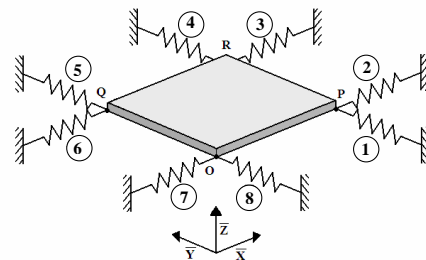
**Fig. 11 Horizontal springs attached to plate**

For static state
The equilibrium results for the values of shear force in the struts at variable b_2 are nearly minimum values from 0.24 to 1.0 for all struts and the values of the moment in strut 1 and 2 are equal from 1.1 to 0.96 but in strut 3 and 4 are equal from 1.2 to 0.8 and have the same direction. The values of the moment and shear force are determined for the asymmetric case analysis using four struts. Figs 12–14 and tables 1–5 show the relation between the variable b_2 vs. the axial load, the moment and the shear force for rigid plate supported by using one strut in each corner but the Figs. 15–17 and the tables 6–9 show the relation between the variable a_2 and b_2 vs. the axial load, the moment and the shear force for rigid plate supported by using one strut in the corners. The rigid plate supported by using two struts in each corner gives the

same equilibrium results of the rigid plate supported by using one strut in each corner.

When the asymmetric plate center of mass c.m. moves in a direction perpendicular to an edge like OP, the struts axial loads (p_1 and p_2 in Fig. 12) and the struts shear forces (q_1 and q_2 in Fig. 13) of this edge increase, but the struts moments (m_1 and m_2 in Fig. 14) decrease than that of the adjacent edge.
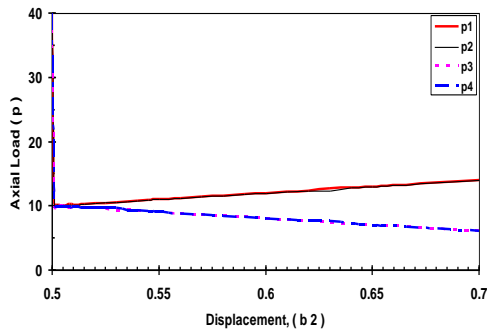
Fig. 12 Struts axial load, p_i vs. b_2 for asymmetric plate case with allowing a lateral motion of the rigid plate by one strut at each corner.
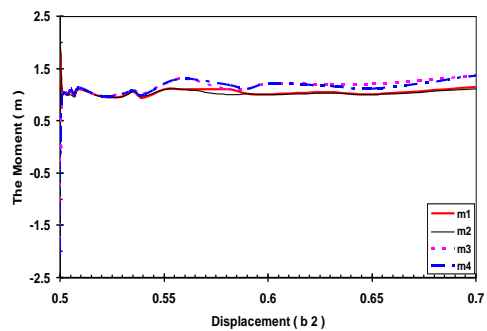
Fig. 13 Struts moment m_1, m_2, m_3, and m_4 vs. b_2 for asymmetric plate case with allowing a lateral motion of the rigid plate by one strut at each corner
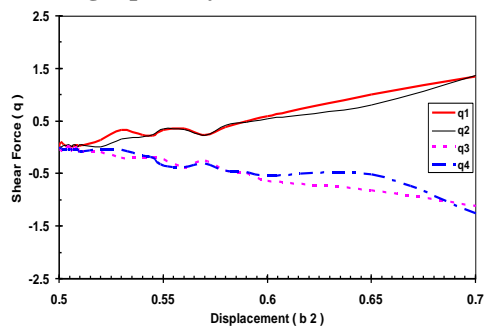
Fig. 14 Struts shear force q_i vs. b_2 for asymmetric plate case with allowing a lateral motion of the rigid plate by one strut.

Table 1 The normal force, the moment, and the shear force at ($a_1 = b_1 = 0.5$)

Strut No.	p	m	q
1	40	2.037	$1.94 * 10^{-06.0}$
2	40	2.037	$1.94 * 10^{-06.0}$
3	40	-2.037	$1.94 * 10^{-06.0}$
4	40	-2.037	$1.94 * 10^{-06.0}$

Table 2 The normal force, the moment, and the shear force at ($b_1 = 0.45$)

Strut No.	P	m	q
1	11	1.1	0.332
2	11	1.1	0.361
3	9	1.2	-0.237
4	9	1.2	-0.360

Table 3 The normal force, the moment, and the shear force at ($b_1 = 0.4$)

Strut No.	P	m	q
1	12	1	0.586
2	12	1	0.544
3	8	1.2	-0.640
4	8	1.2	-0.556

Table 4 The normal force, the moment, and the shear force at ($b_1 = 0.35$)

Strut No.	P	m	q
1	13	1	0.999
2	13	1	0.817
3	7	1.2	-0.829
4	7	1.1	-0.527

Table 5 The normal force, the moment, and the shear force at ($b_1 = 0.3$)

Strut No.	p	m	q
1	14	1.14	1.35
2	14	1.12	1.38
3	6	1.36	-1.13
4	6	1.36	-1.26
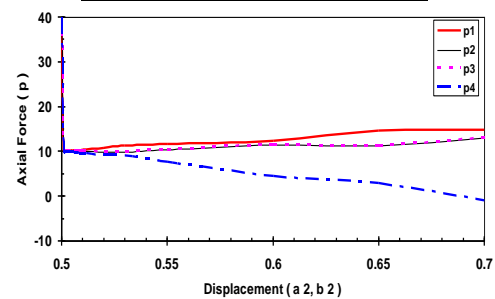
Fig. 15 Struts axial load p_i vs. a_2 and b_2 for asymmetric plate case with allowing a lateral motion of the rigid plate by two struts at each corner.
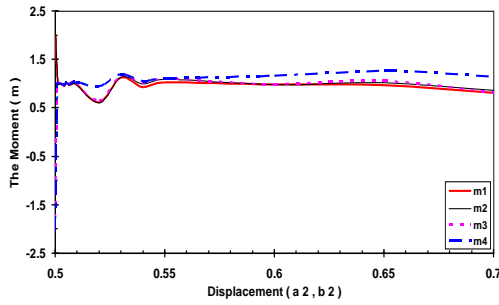
Fig. 16 Struts moment m_1, m_2, m_3, and m_4 vs. a_2 and b_2 for asymmetric plate case with allowing a lateral motion of the rigid plate by two struts at each corner
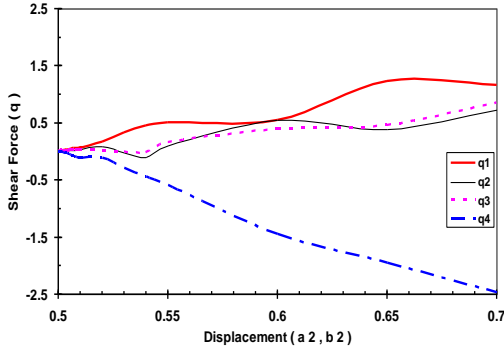
Fig. 17 Struts shear force q_1, q_2, q_3, and q_4 vs. a_2 and b_2 for asymmetric plate case with allowing a lateral motion of the rigid plate by two struts at each corner

Table 6 The normal force, the moment, and the shear force at (a_1= b_1= 0.45)

Strut No.	p	m	q
1	11.58	1.03	0.509
2	10.42	1.1	0.104
3	10.42	1.1	0.160
4	7.53	1.1	-0.589

Table 7 The normal force, the moment, and the shear force at (a_1=b_1= 0.4)

Strut No.	p	m	q
1	12.444	0.987	0.548
2	11.556	0.988	0.557
3	11.556	0.980	0.384
4	4.444	1.155	-1.453

Table 8 The normal force, the moment, and the shear force at (a_1=b_1= 0.35)

Strut No.	p	m	q
1	14.6	0.963	1.236
2	11.3	1.031	0.383
3	11.3	1.051	0.453
4	2.8	1.252	-1.961

Table 9 The normal force, the moment, and the shear force at (a_1=b_1= 0.3)

| Strut No.	p	m	q
1	14.9	1.14	1.35
2	13.1	1.12	1.38
3	13.1	1.36	-1.13
4	-1.1	1.36	-1.26

For dynamic state

The first case to be analyzed is the case where the center of mass is positioned at several points along a line that runs through the center of the plate perpendicular to the edge OP of the plate, as shown in figure (10-a). For this case, the plate moves with three degrees of freedom, i.e., the plate will move vertically, horizontally and/or rotate at an angle θ about the X-axis when the system is subjected to a base excitation. In this analysis, the distance a_1 is fixed at 0.5 and the distance b_1 is varied from 0.45 to 0.3 in increments of 0.05. Note that as b_1 decreases, the eccentricity of the weight increases.

From the solution of the equations of motion, the transmissibility TR is calculated for various excitation frequencies ω. When observing the transmissibility plots in figures (18-19), this looks analogous and the transmissibility is plotted for non-dimensional frequencies ranging from 0.01 to 200. On each plot, the results from the analysis of the asymmetric case (i.e., Case 1) are included so that it is easy to see how the transmissibility changes for various eccentricities. For example, Fig. 18, it has six significant frequency peaks and they each have frequencies ω= 0.89, 10, 15.8, 47, 63.096 and 158.48, from about 0.01 to 0.8 and 1 to 9 the transmissibility is well below unity.

As observed at the higher frequencies, more peaks in the curve start to appear for the lower values of b_1. However, most of these peaks after frequency 9 are higher than the transmissibility of 1.0. The peaks before the frequency of 9 have the transmissibility of lower than 1.0 and are not of much concern because this means the displacement of the plate is much less than the displacement of the base at low frequency (less than 9), which is the desired condition for an effective vibration isolator. Fig. 18 shows the transmissibility vs. frequency for a general case of the position of asymmetric plate center of mass c.m. with a_1=0.5, b_1=0.45. Fig. 19 shows the transmissibility vs. frequency for different values of b_1 for asymmetric plate which supported with one strut at each corner.
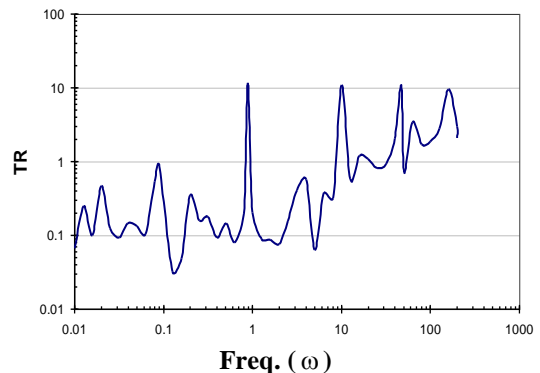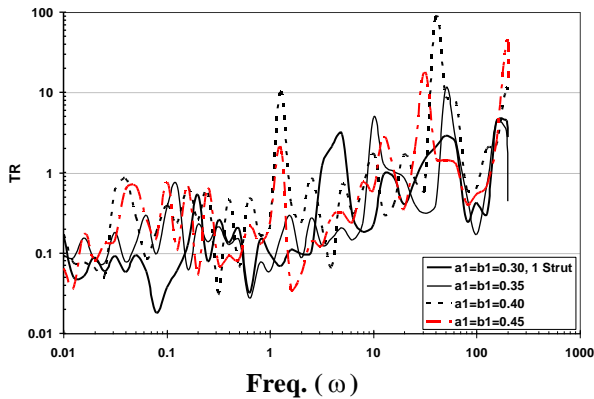

Fig. 18 Transmissibility vs. frequency for asymmetric plate case with allowing a lateral motion of the rigid plate by one strut at each corner, case (a_1=0.5, b_1 = 0.45)

22
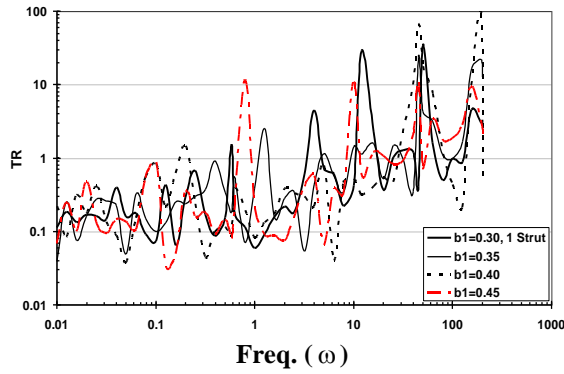
Fig. 19 Transmissibility vs. frequency for different values of b1 for asymmetric plate case with allowing a lateral motion of the rigid plate by one strut in each corner (case 1)

The second case to be analyzed is the case where the center of mass is positioned at several points along a line that runs diagonally from corner R to corner O, as shown in Fig. 10-b. Because of symmetry, it is expected that isolators 2 and 3 will behave identically for this case. In order to analyze this case, the variables a_1 and b_1 will be set equal to each other and will be varied from 0.45 to 0.3 in increments of 0.05. Notice that, as a_1 and b_1 decrease, the eccentricity of the weight increases. Fig. 20 shows the transmissibility vs. frequency for different values of $a_1 = b_1$ for asymmetric plate which supported by one strut at each corner.

Fig. 20 Transmissibility vs. frequency for different values of a1=b1 for asymmetric plate case with allowing a lateral motion of the rigid plate by one strut at each corner (case 2)

Figure 22 shows the transmissibility vs. frequency for the asymmetric plate (case 1) with allowing a lateral motion of the rigid plate supported by using two struts at each corner as shown in Fig. 21.

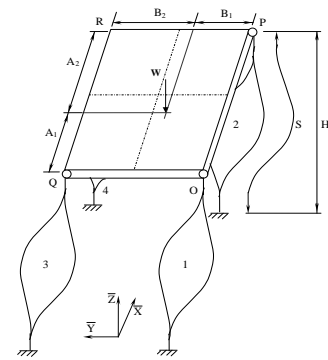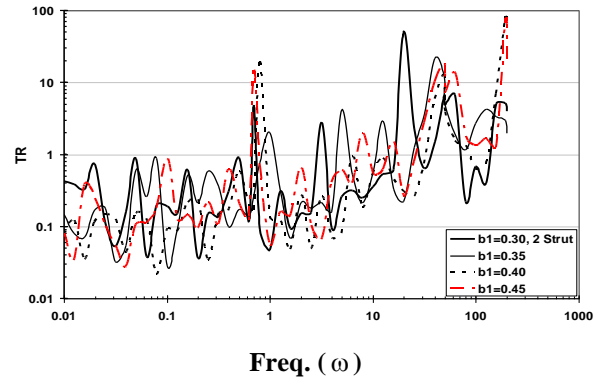**Fig. 21 Eight struts supporting of an asymmetric rigid plate**

Fig. 22 Transmissibility vs. frequency for different values of b1 for asymmetric plate case with allowing a lateral motion of the rigid plate by two struts at each corner (case 1)

Figure 23 shows the transmissibility vs. frequency for the asymmetric rigid plate (case 2) with allowing a lateral motion of the rigid plate supported by using two struts at each corner. Fig. 24 shows the location of the center of mass of asymmetric rigid plate for case 3. By calculating the transmissibility versus random a_1 and b_1 of asymmetric rigid plate which is supported by pair pre-bent struts at each corner, the results obtained have the same behavior as before (Fig. 25).
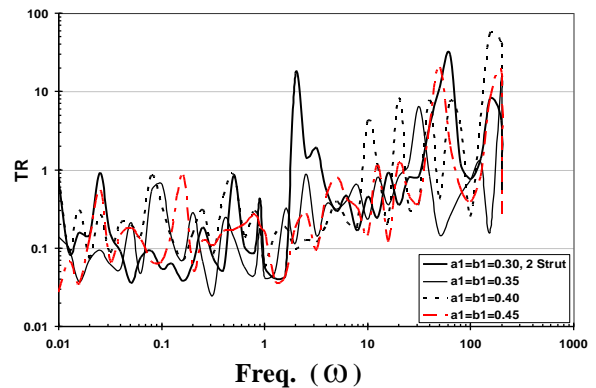
Fig. 23 Transmissibility vs. frequency for different values of a1=b1 with allowing a lateral motion of the asymmetric rigid plate by two struts at each corner (case 2)

23
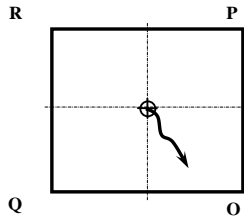
Fig. 24 Location trace of the center of mass of the rigid plate (case 3)

Figures 19, 20, and 25 have similar characteristics, i.e. the transmissibility has peaks values of lower than 1.0 at lower frequencies up to ω =1 and it has peaks values higher than 1.0 at frequencies higher than ω =1.

Fig. 25 Transmissibility vs. frequency for random values of a1 and b1 with allowing a lateral motion of the asymmetric rigid plate by two struts at each corner

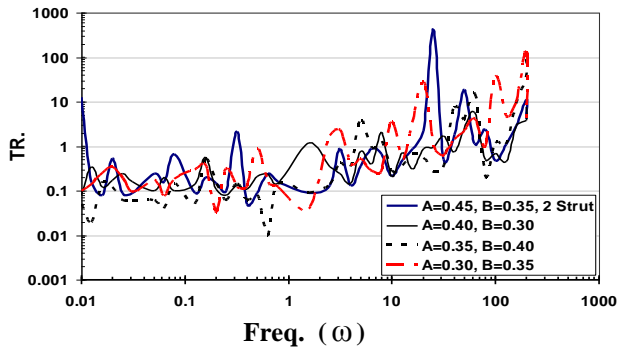In general, it can be observed that the transmissibility values will be better by using two struts than one strut at low frequencies with lateral motion. This method is not recommended to be used in high frequencies for asymmetric plate.

Table 10 shows the peak frequencies of vibrations with allowing lateral motion, and location of the center of mass from one side, (first case-b_1), for asymmetric rigid plate supported by one strut at each corner. Table 11 shows the peak frequencies of vibrations with allowing lateral motion and location of the center of mass from one side, (first case-b_1), for asymmetric rigid plate supported by two struts at each corner. Table 12 shows the peak frequencies of vibrations with allowing lateral motion and Location of the center of mass from two side, (second case-a_1 and b_1), for asymmetric rigid plate supported by one strut at each corner. Table 13 shows the peak frequencies of vibrations with allowing lateral motion and Location of the center of mass from two side, (second case-a_1 and b_1), for asymmetric rigid plate supported by two struts at each corner

Table 14 shows the transmissibility of vibrations with allowing lateral motion, and location of the center of mass from one side, (first case-b_1), for asymmetric rigid plate supported by one strut at each corner. Table 15 shows the transmissibility of vibrations with allowing

lateral motion and location of the center of mass from one side, (first case-b_1), for asymmetric rigid plate supported by two struts at each corner. Table 16 shows the transmissibility of vibrations with allowing lateral motion and location of the center of mass from two sides, (second case-a_1 and b_1), for asymmetric rigid plate supported by one strut at each corner. Table 17 shows the transmissibility of vibrations with allowing lateral motion and location of the center of mass from two sides, (second case-a_1 and b_1), for asymmetric rigid plate supported by two strut at each corner.

Table 18 shows the peak frequencies of vibrations with allowing lateral motion and Location of the Center of Mass from two side, random, (third case-a1 and b1), for asymmetric rigid plate supported by two struts at each corner. Table 19 shows the transmissibility of vibrations with allowing lateral motion and Location of the Center of Mass from two sides, random, (third case-a1 and b1), for asymmetric rigid plate supported by two struts at each corner.

Table 10 Peak frequencies vs. different values of b_1 for asymmetric plate supported by one strut at each corner

a_1	b_1	ω_1	ω_2	ω_3	ω_4	ω_5	ω_6
0.5	0.45	0.89	10.0	15.8	47.0	63.1	158.5
0.5	0.40	0.19	48.0	199	-----	-----	------
0.5	0.35	1.26	5.0	9.9	25.1	47.0	199.5
0.5	0.30	0.58	4.0	12.0	31.6	50.0	155.0

Table 11 Peak frequencies vs. different values of b_1 for asymmetric plate supported by two struts at each Corner

a_1	b_1	ω_1	ω_2	ω_3	ω_4	ω_5	ω_6
0.5	0.45	0.70	7.9	15.8	45.0	63.1	199
0.5	0.40	0.90	49.0	199.5	-----	-----	----
0.5	0.35	1.00	5.0	12.6	39.8	158.4	----
0.5	0.30	0.70	3.16	19.9	49.0	63.1	193

Table 12 Peak frequencies vs. different values of a_1 and b_1 for asymmetric plate supported by one strut at each corner

a_1	b_1	ω_1	ω_2	ω_3	ω_4	ω_5	ω_6
0.45	0.45	1.2	12.5	31.6	195	---	----
0.40	0.40	1.2	10.0	19.9	39.8	199	----
0.35	0.35	10.0	50.1	158.	----	----	----
0.30	0.30	5.0	50.1	195	----	----	----

Table 13 Peak frequencies vs. different values of a_1 and b_1 for asymmetric plate supported by two struts at each corner

a_1	b_1	ω_1	ω_2	ω_3	ω_4	ω_5	ω_6
0.45	0.45	12.6	19.9	50.1	195.0	-----	----
0.40	0.40	10.0	19.9	39.8	63.1	155.	----
0.35	0.35	31.6	125.8	199.5	------	----	----
0.30	0.30	31.6	63.1	155.	-----	----	----

24

Table 14 Transmissibility vs. different values of b_1 for asymmetric plate supported by one strut in each corner

a_1	b_1	TR_1	TR_2	TR_3	TR_4	TR_5	TR_6
0.5	0.45	11.64	10.92	1.21	10.70	3.43	9.49
0.5	0.40	1.45	67.92	94.36	-----	-----	-----
0.5	0.35	2.49	1.15	1.41	1.48	23.45	22.05
0.5	0.30	1.56	4.51	29.14	1.27	34.61	4.59

Table 15 Transmissibility vs. different values of b_1 for asymmetric plate supported by two struts in each corner

a_1	b_1	TR_1	TR_2	TR_3	TR_4	TR_5	TR_6
0.5	0.45	14.47	1.95	1.49	18.30	13.57	75.13
0.5	0.40	19.49	13.04	80.34	-----	------	------
0.5	0.35	2.03	4.17	2.89	21.64	3.37	------
0.5	0.30	4.88	2.77	50.29	6.58	6.70	5.12

Table 16 Transmissibility vs. different values of a_1 and b_1 for asymmetric plate supported by one strut in each corner

a_1	b_1	TR_1	TR_2	TR_3	TR_4	TR_5	TR_6
0.45	0.45	2.04	2.76	17.97	43.3	-----	----
0.40	0.40	10.25	1.72	1.69	85.09	11.42	----
0.35	0.35	4.83	11.05	4.25	-----	------	----
0.30	0.30	2.99	2.87	4.53	-----	------	----

Table 17 Transmissibility vs. different values of a_1 and b_1 for asymmetric rigid plate supported by two struts at each corner

a_1	b_1	TR_1	TR_2	TR_3	TR_4	TR_5	TR_6
0.45	0.45	1.15	1.18	20.38	17.45	-----	----
0.40	0.40	4.12	8.27	7.73	7.29	53.75	----
0.35	0.35	6.41	1.245	14.90	-----	-----	----
0.30	0.30	1.94	29.99	8.18	-----	-----	----

Table 18 Peak frequencies vs. random values of a_1 and b_1 for asymmetric rigid plate supported by two struts at each corner

A_1	b_1	ω_1	ω_2	ω_3	ω_4	ω_5	ω_6
0.45	0.35	0.01	0.32	25.11	50.11	199.5	----
0.40	0.30	1.58	7.94	31.62	63.09	199.5	----
0.35	0.40	5.01	7.94	39.81	63.09	100	200
0.30	0.35	3.16	10	19.95	63.9	100	199.5

Table 19 Transmissibility vs. random values of a_1 and b_1 for asymmetric rigid plate supported by two struts at each corner

a_1	b_1	TR_1	TR_2	TR_3	TR_4	TR_5	TR_6
0.45	0.35	12.57	2.15	432	18.8	11.26	----
0.40	0.30	1.17	2.03	1.66	5.8	3.86	----
0.35	0.40	3.65	1.3	7.2	14.54	1.17	92.5
0.30	0.35	2.31	3.56	26.87	4.16	37.47	140.26

5. Conclusions

The proposed isolation device has the ability to support a relatively large static load with a relatively small static deflection than the traditional vibration isolators and offers a low axial resistance under dynamic excitation, making it ideal for isolating vertical vibrations. By examining the results of model described, the following conclusions can be drawn:

- The use of post-buckled struts as vibration isolators provides a wide range of frequencies at which the transmissibility is well below unity,
- The direction of the horizontal deflection of the buckled struts, whether left direction or right direction, has no effect on the equilibrium moment and shear force and in turn on the transmissibility.
- Tuned isolators can provide improved vibration isolation, even lateral motion is allowed.
- The transmissibility does differ substantially in shape. This is true if lateral motion is allowed or not. However, lateral motion improves the magnitude of transmissibility, and respectively the efficiency of vibration isolation, especially at low frequencies.
- The transmissibility values will be better by using two struts than one strut at low frequencies with lateral motion. This method is not recommended to be used in high frequencies for asymmetric plate.
- The transmissibility at versus random a1 and b1 of asymmetric rigid plate which is supported by pair pre-bent struts at each corner, the results obtained have the same behavior of before calculating, (case 1, and case 2).
- The position of the asymmetric plate center of mass c.m. has a significant effect on the struts axial loads, shear forces, moments, and transmissibility values.

List of symbols

- Its worth to mention that capital letters are denoted to dimensional variables, while small letters are thought for normalized non dimensional quantities. The dimensional and dimensionless variables used in the present paper are:

- A_1 Distance from plate center gravity to strut 1 and strut 3 in $\overline{X}$ -direction (m)
- a_1 Dimensionless distance from plate center gravity to strut 1 and strut 3 in $\overline{X}$ -direction (-)
- A_2 Distance from plate center gravity to strut 2 and strut 4 in $\overline{X}$ -direction (m)
- a_2 Dimensionless distance from plate center gravity to strut 2 and strut 4 in $\overline{X}$ -direction (-)
- A_b Surface area of the block (m^2)
- a_b Dimensionless surface area of the block (-)
- A_p Surface area of the plate (m^2)
- a_p Dimensionless surface area of the plate (-)

- B_1 Distance from plate center gravity to strut 1 and strut 2 in $\overline{Y}$-direction (m)
- b_1 Dimensionless distance from plate center gravity to strut 1 and strut 2 in $\overline{Y}$- direction (-)
- B_2 Distance from plate center gravity to strut 3 and strut 4 in $\overline{Y}$-direction (m)
- b_2 Dimensionless distance from plate center gravity to strut 3 and strut 4 in $\overline{Y}$-direction (-)
- C External damping coefficient per unit length of strut (N.s/m)
- c Dimensionless external damping coefficient per unit length of strut (-)
- C^c Distance from bottom plate surface to C.G. of the plate (m)
- c^c Dimensionless distance from bottom plate surface to C.G. of the plate (-)
- d Subscript used to indicate variables resulting from dynamic analysis
- D_d Depth of the block (m)
- d_d Dimensionless depth of the block (-)
- dS Infinite small length element along the arc of the strut (m)
- ds Dimensionless infinite small length element along the arc of the strut (-)
- dS_i Infinite small length element along the arc of the strut in the ith isolator (m)
- ds_i Dimensionless small element of length along the arc of the strut in the ith isolator (-)
- dX Projection of dS in the $\overline{X}$-direction (m)
- dx Dimensionless projection of ds in $\overline{X}$-direction (-)
- $dX_{i,st}$ projection of dS_i in $\overline{X}$-direction (m)
- $dx_{i,st}$ Dimensionless projection of ds_i in $\overline{X}$-direction (-)
- dY Projection of dS in $\overline{Y}$-direction (m)
- dy Dimensionless projection of ds in $\overline{Y}$-direction (-)
- $dY_{i,st}$ Projection of dS_i in the $\overline{Y}$-direction (m)
- $dy_{i,st}$ Dimensionless projection of ds_i in the $\overline{Y}$-direction (-)
- E Modulus of elasticity of elastic material of strut (assumed to be the same for all struts) (GPa)
- g Gravity acceleration (m/s^2)
- H_o Height of plate from the base, the equilibrium height (m)
- h_o Dimensionless height of plate from the base, the equilibrium height (-)
- H_1 Thickness of the plate (m)
- h_1 Dimensionless thickness of the plate (-)
- H_2 Thickness of the block (m)
- h_2 Dimensionless thickness of the block (-)
- i ☐ The isolator counter ranging from 1…4 (-)

- I Moment of inertia of strut cross-section about the axis of bending (assumed to be the same for all struts) (m^4)
- $\overline{I}_P$ Inertia dyadic
- I_x Principal mass moments of inertia about $\overline{X}$-axis through center of mass (kg.m^2)
- i_x Dimensionless principal mass moments of inertia about $\overline{X}$-Axis through center of mass (-)
- I_Y Principal mass moments of inertia about $-\overline{Y}$-axis through center of mass (kg.m^2)
- i_y Dimensionless principal mass moments of inertia about $-\overline{Y}$-axis through center of mass (-)
- j Number of the horizontal springs (-)
- K Spring stiffness (N/m)
- k Dimensionless spring stiffness (-)
- K_j Stiffness of the eight horizontal attached to the plate, j=1:8 (N/m)
- k_j Dimensionless stiffness of the eight horizontal attached to the plate, j=1:8 (-)
- L Length of strut (m)
- M Bending moment acting on the strut (N.m)
- m Dimensionless bending moment acting on the strut (-)
- M_1 Plate mass (kg)
- m_1 Dimensionless plate mass (-)
- M_2 Block mass (kg)
- m_2 Dimensionless block mass (-)
- $M_{i,st}$ Bending moment acting on the strut for the ith isolator (N.m)
- $m_{i,st}$ Dimensionless bending moment acting on the strut for the ith isolator (-)
- P Horizontal component of force acting on the strut at S = 0 (N)
- p Dimensionless horizontal component of force acting on the strut at s=0 (-)
- $P_{i,st}$ Component of force acting in $\overline{X}$-direction on the strut for the ith isolator (N)
- $p_{i,st}$ Dimensionless component of force acting in $\overline{X}$-direction on the strut for the ith isolator (-)
- P_o Applied load from the rigid plate on the strut, (the classical Euler critical load, P_{cr}) (N)
- p_o Dimensionless applied load from the rigid plate on the strut, (the classical Euler critical load, P_{cr}) (-)
- P_w Ratio of the weight W to the weight of the strut µgl (-)
- Q Vertical component of force in the strut at S = 0 (N)
- q Dimensionless vertical component of force in the strut at s = 0 (-)
- $Q_{i,st}$ Component of force acting in $\overline{Y}$-Direction on the strut in the ith isolator (N)
- $q_{i,st}$ Dimensionless component of force acting in $\overline{Y}$-Direct. on the strut in the ith isolator (-)
- S Arc length of the strut (m)

26

- s Dimensionless arc length of the strut (-)
- st Subscript used to indicate variables which result from the static equilibrium analysis (-)
- T   Time (s)
- t Dimensionless time (-)
- U_o Peak or maximum displacement (i.e. the amplitude) of the point from a datum line (m)
- u_o Dimensionless peak or maximum displacement (i.e. the amplitude) of the point from a datum line (-)
- U(T) Position of the point with respect to time T (m)
- u(t) Dimensionless position of the point with respect to time t (-)
- $V_{s,i}$ Potential energy in the springs (N)
- W   Weight of the supported load (full rigid plate) (N)
- w Dimensionless weight of the supported load (-)
- W_d Width of the block (m)
- w_d Dimensionless width of the block (-)
- Yo   Initial buckling of the strut (m)
- y_o Dimensionless initial buckling of the strut (-)
- Y_{L1} Strut 1 $\overline{Y}$ -lateral movement (m)
- y_{L1} Dimensionless strut 1 $\overline{Y}$ - lateral movement (-)
- Y_{L2} Strut 2 $\overline{Y}$ -lateral movement (m)
- y_{L2} Dimensionless strut 2 $\overline{Y}$ - lateral movement (-)
- Y_{L3} Strut 3 $\overline{Y}$ -lateral movement (m)
- y_{L3} Dimensionless strut 3 $\overline{Y}$ - lateral movement (-)
- Y_{L4} Strut 4 $\overline{Y}$ -lateral movement (m)
- y_{L4} Dimensionless strut 4 $\overline{Y}$ - lateral movement (-)
- Y_{b1} Strut 1 $\overline{Y}$ - buckling movement (m)
- y_{b1} Dimensionless strut 1 $\overline{Y}$ - buckling movement (-)
- Y_{b2} Strut 2 $\overline{Y}$ - buckling movement (m)
- y_{b2} Dimensionless strut 2 $\overline{Y}$ - buckling movement (-)
- Y_{b3} Strut 3 $\overline{Y}$ - buckling movement (m)
- y_{b3} Dimensionless strut 3 $\overline{Y}$ - buckling movement (-)
- Y_{b4} Strut 4 $\overline{Y}$ - buckling movement (m)
- y_{b4} Dimensionless strut 4 $\overline{Y}$ - buckling movement (-)
- $\widetilde{Z}$ Distance between centre of each area and OPRQ surface area (m)
- $\widetilde{z}$ Dimensionless distance between centre of each area and OPRQ surface area (-)
- α   Aspect ratio of the plate (-)
- $β_i$ The ith isolator factor for strut stiffness modification (-)

- $θ_{i,st}$ Angle of the deflected strut in the ith isolator measured from $\overline{X}$ -axis [o]
- $θ_o$ initial angle [o]
- μ Mass per unit length of the strut (kg/m)
- μ Dimensionless mass per unit length of the strut (-)
- $\overline{ω}_P$ Angular velocity vector (sec^{-1})
- Ω   Applied frequency of the axial excitation of the strut base (sec^{-1})
- ω   Dimensionless applied frequency of the axial excitation of the strut base (-)

References

[1]- Alloway, L.A.: Analysis of buckled columns and rigid-link mechanisms used as vibration isolators. M. E. Report, Virginia Tech (2003)

[2]- Bai, M.R. and LIU, W.: Control design of active vibration isolation using μ-synthesis. J. Sound Vib. 257(1), pp.157-175, doi:10.1006/jsvi.5036 (2002)

[3]- Britvec, S.J.: The Stability of Elastic Systems. p. 190, Pergamon Unified Engineering Series, Oxford (1973)

[4]- Carrellaa, A., Brennana, M.J., Kovacicb, I., and Waters, T.P.: On the force transmissibility of a vibration isolator with quasi-zero-stiffness. J. Sound Vib. 322, pp.707–717, doi:10.1016/j.jsv. 2008.11.034 (2009)

[5]- Carrellaa, A., Brennana, M.J., Watersa, T.P, Shin, K.: On the design of a high-static–low-dynamic stiffness isolator using linear mechanical springs and magnets. J. Sound Vib. 315, pp.712–720, doi:10.1016/j.jsv.2008.01.046 (2008)

[6]- Chopra, A. K.,: Dynamics of Structures-Theory and Applications to Earthquake Engineering. 2nd edn, Prentice Hall, Upper Saddle River, New Jersey, 01 (2001)

[7]- Den Hartog, J.P.: Mechanical vibrations. Dover Publications, New York (1985)

[8]- El-Kafrawy, A. et al.: Vibration isolation of a symmetric and asymmetric rigid bar using struts subject to axial static and dynamic excitation. Proc. IMechE Vol. 225, Part C, pp.334-346, DOI:101243 /09544062JMES2125 (4 May 2010)

[9]- El-Kafrawy, A. et al.: (28 September 2010) Vibration isolation of a symmetric rigid plate using struts subject to axial static and dynamic excitation. Int. J. Mech. Mater Des, DOI 10.1007/s10999-010-9135-1, Springer (28 September 2010)

[10]- Hoque, M.E., Mizuno, T., Ishino, Y., and Takasaki, M.: A six-axis hybrid vibration isolation system using active zero-power control supported by passive weight support mechanism. J. Sound Vib. 329 pp.3417–3430, doi:10.1016/j.jsv.2010.03.003 (2010)

[11]- Inman, D.J.: Engineering vibration. Prentice-Hall, Englewood Cliffs, NJ. Jalili, N., A new perspective

27

for semi-automated structural vibration control (1994)

[12]- Jalili, N.: A new perspective for semi-automated structural vibration control. J. Sound Vib. 238(3), pp.481-494, doi:10.1006/jsvi.2000.3210 (2000)

[13]- Jeffers, A.E., Plaut, R.H., and Via, C.E.: Vibration isolation of a horizontal rigid plate supported by Pre-bent Struts. Blacksburg, VA, December (2005)

[14]- Lee, C.M., Goverdovskiy, V.N., Temnikov, A.I.: Design of springs with ''negative'' stiffness to improve vehicle driver vibration isolation. J. Sound Vib. 302 pp.865–874, doi:10.1016/j.jsv.2006.12.024 (2007)

[15]- Leo, D.J. and Inman, D.J.: A quadratic programming approach to the design of active-passive vibration isolation systems. J Sound Vib. 220(5), pp.807-825, Article No. jsvi.1998.1937 (1999)

[16]- Mizuno, T., Takasaki, M., Kishita, D., Hirakawa, K.: Vibration isolation system combining zero-power magnetic suspension with springs. Control Engineering Practice 15, pp.187–196, doi:10.1016/j.conengprac.2006.06.001 (2007)

[17]- Plaut, R.H., Alloway, L.A., and Virgin, L.N. : Nonlinear oscillations of a buckled mechanism used as a vibration isolator. In: Proceedings of the IUTAM Symposium on Chaotic Dynamics and Control of Systems and Processes in Mechanics, Rome, Italy, Vol.122, 241-250 (2003)

[18]- Sidbury, J.E.: Analysis of buckled and pre-bent columns used as vibration isolators, M.Sc. Thesis, Virginia Polytechnic Institute and State University, Blacksburg, VA, (2003)

[19]- Virgin, L.N.: The dynamics of symmetric post-buckling. Int. J. Mech. Sci. 27, 235–248, (1985)

[20]- Virgin, L.N., Davis, R.B.: Vibration isolation using buckled struts. J. Sound and Vib. 260, 965–973 (2003)

[21]- Wolfram Research, Inc.: Mathematica, Version 5.2.0.0. Champaign, IL 61820 USA (2005)